IN-SITU OBSERVATION OF HYDRO-SEDIMENT DYNAMICS ON STEEPLY SLOPING SEABED IN DEEP WATER

Takenori Shimozono, University of Tokyo, shimozono@coastal.t.u-tokyo.ac.jp
Takashi Yamano, Toyo Construction Co.,Ltd., yamano-takashi@toyo-const.co.jp
Yoshimitsu Tajima, University of Tokyo, yoshitaji@coastal.t.u-tokyo.ac.jp

INTRODUCTION

Evaluating the local sediment balance is a crucial component of effective coastal erosion management. Traditionally, we set a depth of closure in a target coastal area, representing the point beyond which sediment transport is assumed to be minimal. This concept helps us maintain the assumption that the sediment budget remains balanced landward. However, during extreme events, sediment transport can exceed this depth, leading to a loss of coastal sediments. This scenario is particularly relevant for coasts adjacent to a steep offshore slope, where sediments released onto the slope may never return to the upper coast. The process of downward sediment transport in the lower shoreface remains poorly understood, primarily due to the inherent challenges associated with in-situ observations of sediment dynamics in deep water.

Our study aims to explore the characteristics of near-bed flows and sediment transport on steep slopes in deep water. We focus on the Fuji Coast, one of Japan's steepest coasts, situated within a deep embayment connecting to the Pacific Ocean, namely Suruga Bay (see Fig. 1a). Coastal erosion and sediment loss to deep water have been persistent issues on the coast. To gather comprehensive data, we conducted an intensive two-month observation during the high-wave season from August to October 2023 on a steep offshore slope as depicted in Fig. 1b. At the observation point, the local bed slope had a ratio of 1:2.6 (equivalent to a 22-degree bed angle), and the water depth was approximately 30 m. Our instrumentation included a variety of devices, such as an Acoustic Doppler Current Profiler (ADCP), an ultrasonic/pressure wavemeter, electromagnetic velocity meters, and a bed level sensor, all securely mounted on a measurement frame anchored to the seabed. Furthermore, we deployed several waterproof cameras on piles anchored to the seabed to capture images of the bed surface from different angles. The analysis of the field dataset collected by these instruments yields valuable insights into the sediment dynamics in deep-water environments.

RESULTS AND DISCUSSION

Figure 2 presents the observed dataset obtained from various instruments. The water depth displayed variations within the range of 29.0 to 30.7 m due to tidal fluctuations (see Fig. 2a). Notably, there were no direct impacts from typhoons during this period, with the maximum significant wave height reaching only 2.0 m (see Fig. 2b). The wave period implies that the high wave peaks were primarily generated by long-period swells originating from the Pacific Ocean (see Fig. 2c). Data from the ADCP revealed intermittent development of strong surface currents aligned in an east-west direction, closely matching the alongshore orientation (see Fig. 2d). In contrast, surface currents in the cross-shore direction (north-south) exhibited a diurnal cycle driven by land-sea breezes. In the lower measurement cell, situated between 1.5 and 3.0 m above the seabed, the counter-currents occasionally developed in the alongshore direction (see Fig. 2e). In contrast, almost no significant mean flow existed in the cross-shore direction.

Similar observations were obtained using the electromagnetic current meter installed approximately 1.0 m above the seabed. The collected data indicates that there was no sustained mean flow capable of inducing significant sediment transport of coarse sand and gravel which are main bed materials in the area. Meanwhile, as depicted in Fig. 2g, the root-mean-square (RMS) velocity data recorded by the electromagnetic current meter over 8-min continuous data reveals the presence of relatively high oscillatory flows induced by long-period swells. The RMS value for the nearbed cross-shore velocity reached the maximum of 0.2 m/s on October 5th, and the maximum instantaneous velocity at this time exceeded 0.5 m/s. Such strong flows are considered capable of transporting sediment grains of gravel to pebble size with the help of the downslope force of gravity. While the specific results are not presented here, it is worth noting that the transfer function, relating water surface elevation to bottom flow velocity within the wave frequency range, closely aligns with the predictions from linear wave theory.

To investigate sediment movement under the observed flows, we analyzed bed-surface images taken by three cameras at 20-minute intervals during the observation period. Daily sequential images were created by selecting a representative image from each day for the camera looking at the sloping bed (see Fig. 3 for an example of bed-surface images). In these images, we set interrogation windows, as illustrated in Fig. 3, and computed cross-correlations of luminance signals within these windows for two sequential image pairs. Cross-correlation values are low when changes occur in the bed-surface structure, particularly when large-sized sediment grains move. The results of this cross-correlation analysis are presented in Fig. 2h, indicating that downslope sediment transport is primarily driven by wave-induced flows associated with long-period swells.

CONCLUSION

Our observations have confirmed that substantial cross-shore sediment transport and subsequent coastal sediment loss occur exclusively when high and prolonged swells reach the coast. Consequently, the annual sediment loss appears to be correlated with the cumulative wave energy over the period during which nearbed flows exceed the threshold for incipient sediment motion. During the upcoming conference, we will provide a more comprehensive analysis regarding the sediment mobility on the steep slope, drawing further insights from our observation dataset.

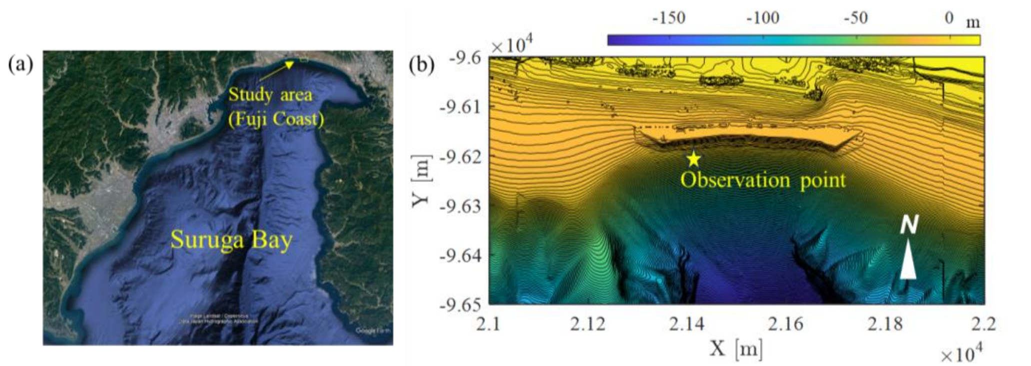

Figure 1 – Overview of the study area: (a) Suruga Bay, (b) Observation point

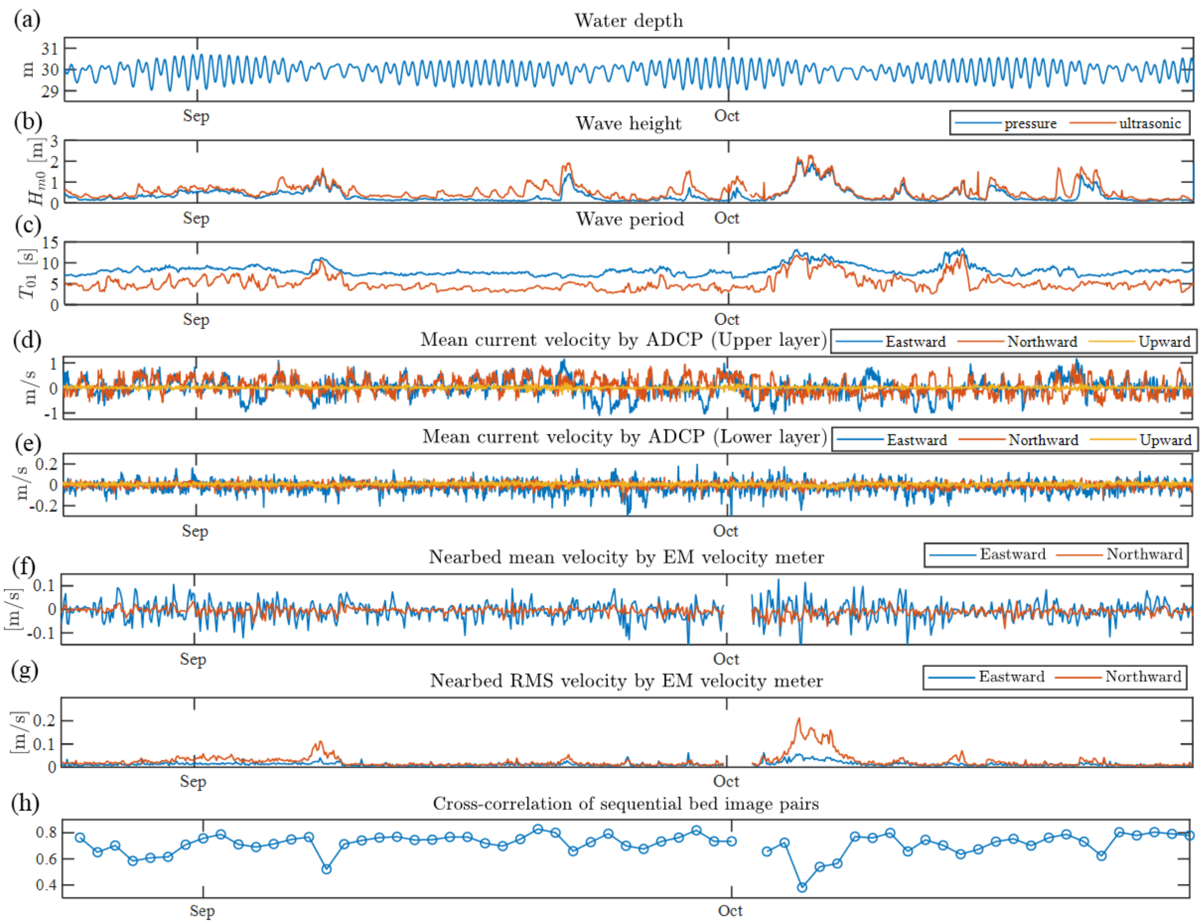

Figure 2 – Observation results from Aug 24 – Oct 27, 2023: (a) water depth, (b) wave height, (c) wave period, (d) surface-layer current velocity (e) lower-layer current velocity, (f) nearbed current velocity, (g) nearbed RMS velocity and (h) cross-correlation of sequential bed-surface image pairs over 1 day (the correlation was taken in the interrogation windows in Figure 3).

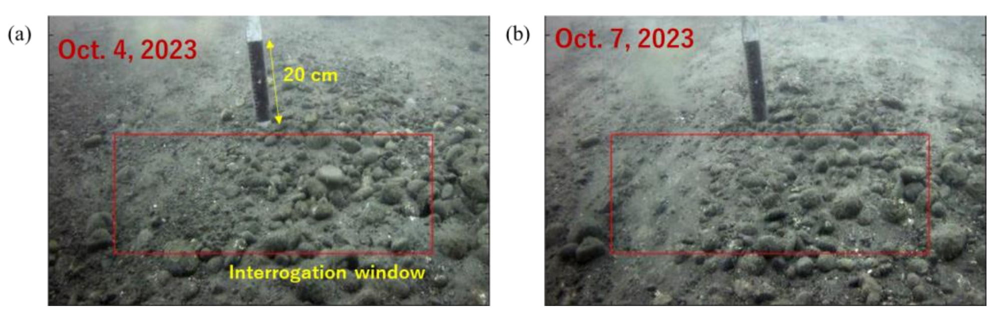

Figure 3 – Bed surface changes captured by a water-proof camera looking upslope.